Available online at www.sciencedirect.com
ScienceDirect
Aerosol Science 37 (2006) 1429–1441
Journal of Aerosol Science
www.elsevier.com/locate/jaerosci

Deposition of fiber in a human airway replica

Wei-Chung Su*, Yung Sung Cheng

Lovelace Respiratory Research Institute, 2425 Ridgecrest Dr. SE, Albuquerque, NM 87108, USA

Received 27 September 2005; received in revised form 23 January 2006; accepted 31 January 2006

Abstract

Fiber is a notorious occupational hazard. Exposures to airborne asbestos fiber in the workplace increase the incidence of lung cancer for asbestos workers. Due to the lack of experimental data, the nature of fiber deposition in the human airway is unclear. In this study, a set of experiments were carried out to investigate the effect of fiber dimension and fiber inertia on the deposition pattern in the human airway replica. The deposition study was conducted by delivering aerosolized carbon fibers into the replica at constant inspiratory flow rates of 15–60 l/min. The results showed that impaction is the dominant deposition mechanism in this study. Most of the high-inertia fibers deposited in the oropharynx and the carina ridges of the bifurcations in tracheobronchial airways. A series of fiber deposition patterns were obtained and the deposition efficiencies were acquired for certain regions in the human airway replica.

Keywords: Fiber; Human airway; Deposition fraction

1. Introduction

Fiber is an elongated particle with a length more than 5 μm and an aspect ratio, β (the ratio of the length to the diameter), over 3 (NIOSH, 1994). The aerodynamic diameter of a fiber depends primarily on its diameter and only slightly on its length (Cheng, Powell, Smith, & Johnson, 1995; Stöber, Flachsbart, & Hochrainer, 1970). Fiber is a notorious occupational hazard. Exposures to airborne asbestos fibers in the workplace increase the incidence of lung cancer, fibrosis, and mesothelioma for asbestos miners and workers. Although the use of asbestos fibers was banned by the US Environmental Protection Agency in 1989, new fiber materials such as man-made vitreous fibers (MMVFs) are being manufactured to replace asbestos for new applications. However, studies conducted in laboratory animals have shown that certain MMVFs may have a biological effect similar to that of asbestos (Hesterberg & Hart, 2001; IARC, 2002; Kamstrup, Ellehauge, Collier, & Davis, 2002). Therefore, it is believed that a potential risk of fiber-related diseases still exists for workers in the MMVF material industry.

There are four mechanisms involved in fibers depositing in a human airway: sedimentation, impaction, diffusion, and interception. Each deposition mechanism is significant in a certain fiber dimension range and insignificant in others. The hazard of exposure to fiber depends strongly upon the localities in the human airway where the fiber deposits as well as the corresponding fiber dimension distribution at these localities (Sussman, Cohen, & Lippmann, 1991). It has been reported that fiber dimensions and biopersistence play an essential role in the pathogenesis of fiber-related lung

* Corresponding author. Tel.: +1 505 348 9571; fax: +1 505 348 8567.
E-mail address: wsu@LRRI.org (W.-C. Su).

0021-8502/$ - see front matter © 2006 Elsevier Ltd. All rights reserved.
doi:10.1016/j.jaerosci.2006.01.015

diseases (Bernstein, Riego Sintes, Ersboell, & Kunert, 2001; Lippmann, 1990; Timbrell, 1982). For example, long and thin fibers have greater toxicity than short and thick fibers. Therefore, by knowing the sites of preferred deposition for fiber in the human airway, and the corresponding dimension distributions of fiber at these sites, it would improve significantly on understanding the etiological process and determining the hazards for fiber-related lung diseases. However, very few experimental studies to date have been conducted on the subject of fiber deposition in the human airway. Ethical constraints also severely limit the use of fibers in human volunteer studies. As a result, the experimental data is extremely limited on this topic. Only one set of experimental data was available (Sussman et al., 1991). This lack of data not only makes the nature of fiber deposition in the human airway remain unknown, but also hampers the verification of available lung deposition models.

In order to fill this gap stated above, the goal of this study is to obtain sufficient experimental data for fiber deposition in a human airway to investigate the deposition pattern, deposition mechanism, and their correlation with the fiber dimension. In this study, realistic human airway replicas were made. These replicas have well-defined airway geometry encompassing the oral cavity to the 4th tracheobronchial bifurcation. A MMVF-like carbon fiber with uniform diameter was chosen as the test material. This fiber material was used for a nasal deposition study in our laboratory (Su & Cheng, 2005) and was proven it provides a simple way for the microscopic measurement of the fiber dimension. Due to the great number of experimental data and deposition information that came from this study, in this paper, attention is focused only on understanding and interpreting the experimental result itself. The comparison of obtained experimental data with published theoretical calculations will be discussed in greater detail in our upcoming publications.

2. Experimental method

2.1. Human airway replica

Physical molds of human airways have been developed (Cheng, Smith, & Yeh, 1997) from in vivo measurements (oral cavity) and cadavers (tracheobronchial section). Human airway replicas produced from these molds have defined geometric dimension; therefore, it is appropriate to use these replicas for correlating the deposition information with airway dimension, and elucidating the deposition mechanism (Cheng et al., 1996). The human airway replica in this study was made from conductive silicone rubber (KE-4576, Shin-Etsu Chemical Co., Ltd., Tokyo, Japan). The use of conductive material can minimize the fiber deposition due to the electrostatic effect. Fig. 1 shows the structure and physical model of the human airway replica. The replica consists of oral cavity, pharynx, larynx, and tracheobronchial airways up to the fourth bifurcation. Prior to the deposition experiment, silicon oil (550 Fluid, Dow Corning Co., Midland, MI) was applied to the inside surface of the replica to simulate the adhesive nature of the viscous mucus layer in a real human airway. Moreover, the oil coating can also force fibers to remain in the place where they originally deposited. Cheng, Zhou, and Chen (1999) and Zhou and Cheng (2005) conducted deposition experiments with spherical particles using the same human airway replica. The results have shown that reliable deposition data could be acquired by using this replica. It is worth noting that, in this study, the dimension of the glottis opening of the replica was modified in different sizes based on the information provided by Martonen and Lowe (1983). Changing the glottis opening allowed the replica to simulate the real situation of human airway under different inspiratory flow rates.

2.2. Test fiber material

The test carbon fiber, provided by Hercules Inc. (Wilmington, DE), are conductive, black in color, monodisperse in diameter (3.66 μm), polydisperse in length, and density measured at 1830 kg/m^3. The test fiber material contains cylindrical fibers and fiber debris. Preliminary investigation showed that the fiber debris is mainly in the 1–5 μm size range and has a number concentration of 27% of the total fiber. The fiber count median length (CML) is 14.83 (σ_g=4.00) and the count median diameter (CMD) is 3.66 (σ_g = 1.11). Both length and diameter distributions are detailed in Su and Cheng (2005). This carbon fiber has been used for a size classification study in our laboratory (Chen, Yeh, & Hobbs, 1993). Using monodisperse-diameter fibers is a new approach in deposition studies since it provides a simple way to obtain fiber dimension (length measurement only) and a sure way to determine the effect of fiber dimension on the deposition pattern and deposition mechanism. In this study, fibers larger than 10 μm were counted as contributing to the deposition data. All fibers with lengths shorter than 10 μm were discarded.

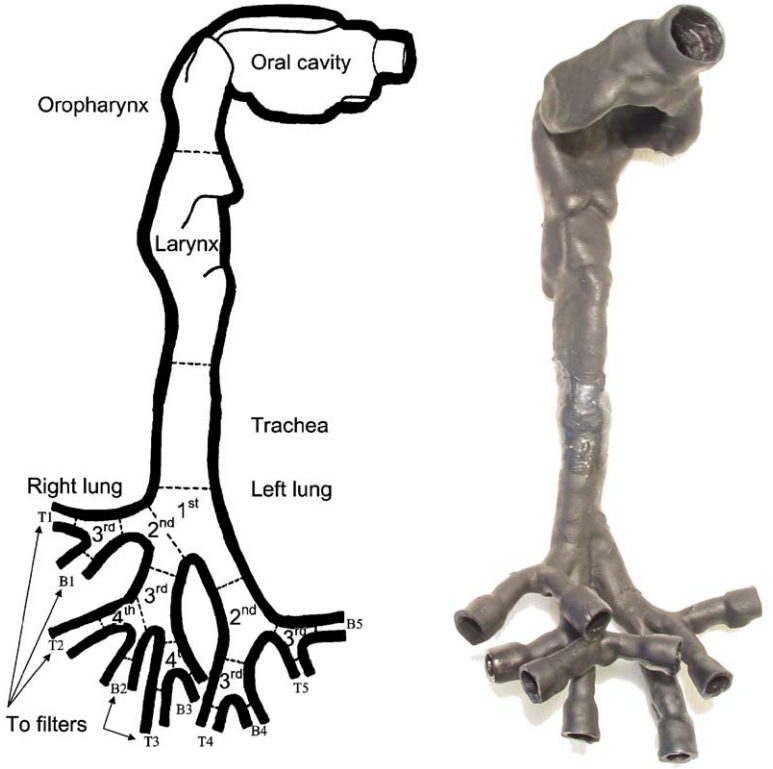

Fig. 1. Structure and regions of the human airway replica.

The aerodynamic diameter (d_{ae}) of a fiber could be calculated by Stöber (1972)

$$d_{ae} = d_{ve}\sqrt{\rho/\rho_o\kappa}, \tag{1}$$

where d_{ve} is the volume equivalent diameter, ρ is the density of a fiber, ρ_o is the density of water, and κ is the dynamic shape factor for a prolate spheroid. For a prolate spheroid flying in the air with its long axis orientating perpendicularly, parallel, and randomly to the flow direction, the dynamic shape factor is $\kappa_\perp$, $\kappa_\parallel$ and κ_r, respectively, and can be calculated in the following equations:

$$\kappa_\perp = \frac{\frac{8}{3}(\beta^2-1)\beta^{-1/3}}{\left((2\beta^2-3)\Big/\sqrt{\beta^2-1}\right)\ln\left(\beta+\sqrt{\beta^2-1}\right)+\beta}, \tag{2}$$

$$\kappa_\parallel = \frac{\frac{4}{3}(\beta^2-1)\beta^{-1/3}}{\left((2\beta^2-1)\Big/\sqrt{\beta^2-1}\right)\ln\left(\beta+\sqrt{\beta^2-1}\right)-\beta}, \tag{3}$$

$$\frac{1}{\kappa_r} = \frac{1}{3\kappa_\parallel} + \frac{2}{3\kappa_\perp}, \tag{4}$$

where β is the fiber aspect ratio, and Eq. (4) is from Willeke and Baron (1993). Based on the above, if a 20-μm-long carbon fiber flies in the air flow with its long axis orientating perpendicular to the flow direction (dynamic shape factor $= \kappa_\perp$), the aerodynamic diameter of this carbon fiber, $d_{ae(\perp)}$, will be 8.4 μm. On the other hand, if the carbon fiber's long axis is parallel to the flow direction (dynamic shape factor $= \kappa_\parallel$), the aerodynamic diameter, $d_{ae(\parallel)}$ is 9.7 μm. However, if the carbon fiber orientates randomly in the air (dynamic shape factor $= \kappa_r$), the aerodynamic diameter, $d_{ae(r)}$ is 8.8 μm. In contrast, for a 150-μm-long carbon fiber in the air, its $d_{ae(\perp)}$, $d_{ae(\parallel)}$, and $d_{ae(r)}$ are 10.9, 13.7, and 11.9 μm, respectively.

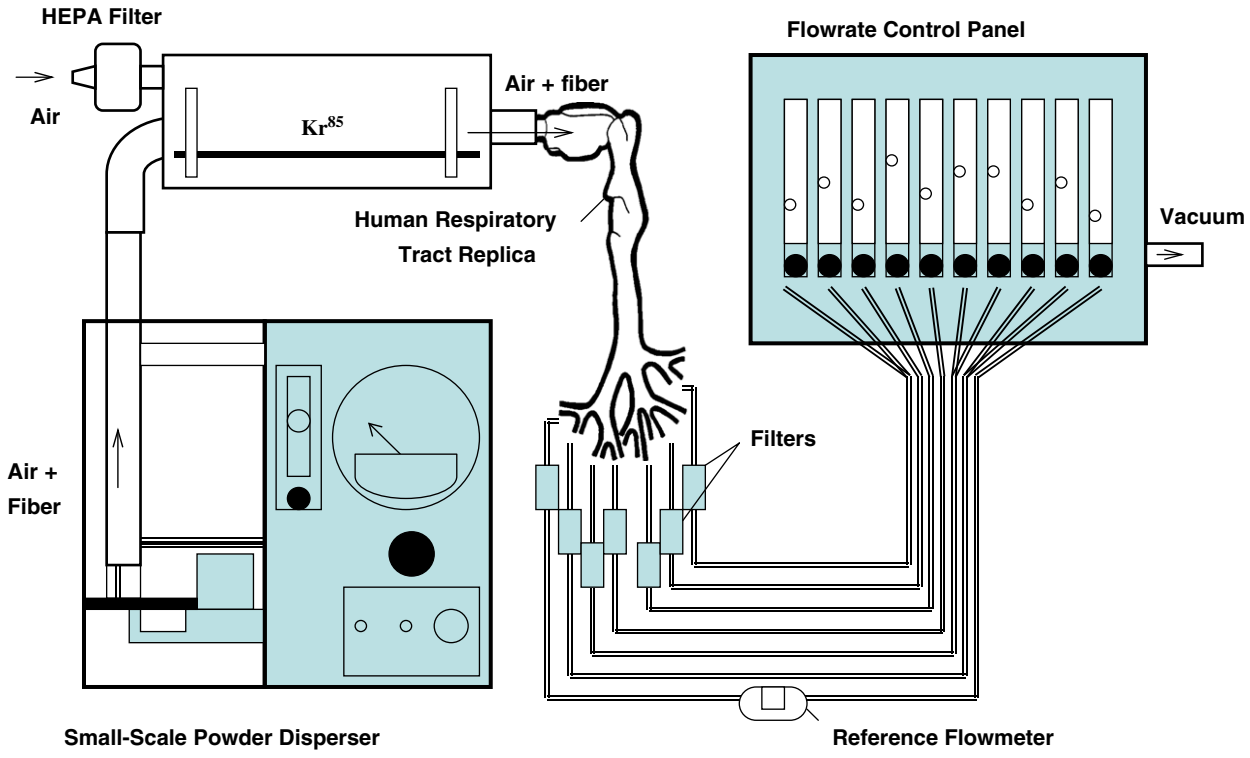

Fig. 2. Schematic diagram of the experimental setup for the fiber deposition study.

Table 1
Flow rate distribution in the bronchial airways for a 43.5 l/min inspiratory flow rate

	Right lung						Left lung			
	Upper		Middle		Lower		Upper		Lower	
Bronchial airways	T1	B1	T2	B2	T3	B3	T4	B4	T5	B5
Branch flow rates (l/min)	4.1	3.9	5.1	8.7	2.6	2.7	4.6	4.7	3.7	3.4

2.3. Experimental setup, sample preparation and fiber measurement

Fig. 2 shows the experimental setup for the fiber deposition study. The experimental apparatus included a fiber generator, a charge neutralizer, the human airway replica, and 10 fiber sampling cassettes. The fiber aerosol was generated by a small-scale powder disperser (Model 3433; TSI Inc., St. Paul, MN). Dispersed fibers were first transferred to a Kr^{85} charge neutralizer, and then delivered into the human airway replica. Fibers impacting on the inside surface of the replica were captured and remained in place due to the silicon oil coating. Ten 25-mm asbestos filter cassettes (Zefon International Inc., Ocala, FL) were attached to the end of each bronchus for collecting fibers that passed through the replica. Each bronchus branch had its own assigned flow rate to make the overall flow distribution similar as described in Cohen, Sussman, and Lippmann (1990) and Sussman et al. (1991). Table 1 shows an example of the flow rate distribution in the bronchial airways. In this study, three inspiratory flow rates (15, 43.5, and 60 l/min) were tested which covered the breathing flow rate range of an adult under different activities (at rest to moderate exercise), and three experiments were conducted for each flow rate in order to obtain an average deposition value. Although the pulsating flow rate is more realistic for the human respiratory scenario, it is widely accepted that the deposition of particles in the human airway occurs primarily while air is inhaled.

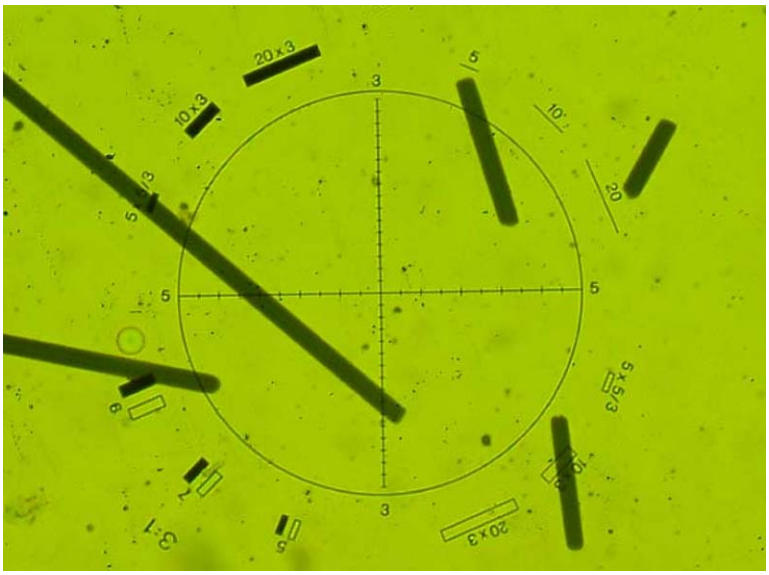

Fig. 3. Fiber counting/measuring with G22 Walton–Beckett graticule (under 400× magnification).

After an experiment, the replica was carefully cut into segments based on the human airway structure. Each segment cut from the replica was put in glass jar or vial containing isopropyl alcohol and placed in an ultrasonic bath for 5 min. The inside surface of the replica was later scraped with a microspatula and flushed with isopropyl alcohol to enhance the removal of deposited fibers. The washed-out alcohol solution was continually agitated so that fibers in the solution were well mixed. The solution was then vacuum-filtered by a filtration assembly with a 25-mm mixed cellulose ester membrane filter (GSWP, Millipore Co., Bedford, MA). Filters taken from the filtration assembly were dried at room temperature in a dust-free environment and then prepared as sample slides for a later microscopic counting/measurement process. In total, 26 sample slides were obtained for each experiment (first bifurcation was subdivided into four segments).

The fiber sample slides were examined by an optical microscope (BH-2; Olympus Optical Co., Tokyo, Japan) with a G22 Walton–Beckett graticule (Pyser-SGI Ltd., Kent, UK). The total number of fibers and the length of individual fibers in the viewing area of the graticule were determined and measured based on NIOSH method 7400. In this way, the fiber length distribution, the average number of fibers in one viewing area, and the total number of fibers for a sample slide could be acquired. Fig. 3 shows an example of fibers in the G22 Walton–Beckett graticule viewing area. In this study, each sample slide was counted/measured for 150 fibers or 150 viewing areas, depending on whichever came first.

3. Results

3.1. Deposition sites

It is known that inhaled fibers as well as other inhaled particles are not distributed uniformly in the human airway. There exist some sites of preferred deposition or "hot spots" in the human airway due to certain deposition mechanisms. In order to investigate the preferred deposition sites, exclusive deposition experiments were conducted using a human airway replica made from white silicone rubber (3145 RTV, Dow Corning Co., Midland, MI). In this way, the preferred deposition sites could be visually examined without difficulty since the color of the test carbon fiber is black and the background (replica) is a light color. Fig. 4 shows four deposition sites for fiber deposition in the human airway with an inspiratory flow rate of 43.5 l/min. As can be seen in Fig. 4a, the region from the oropharynx to the larynx in the upper airway is one of the preferred deposition sites. In the lower airway, Figs. 4b–d show that the carina in each tracheobronchial bifurcation is the site of preferred deposition. Fibers were easily observed to deposit and accumulate

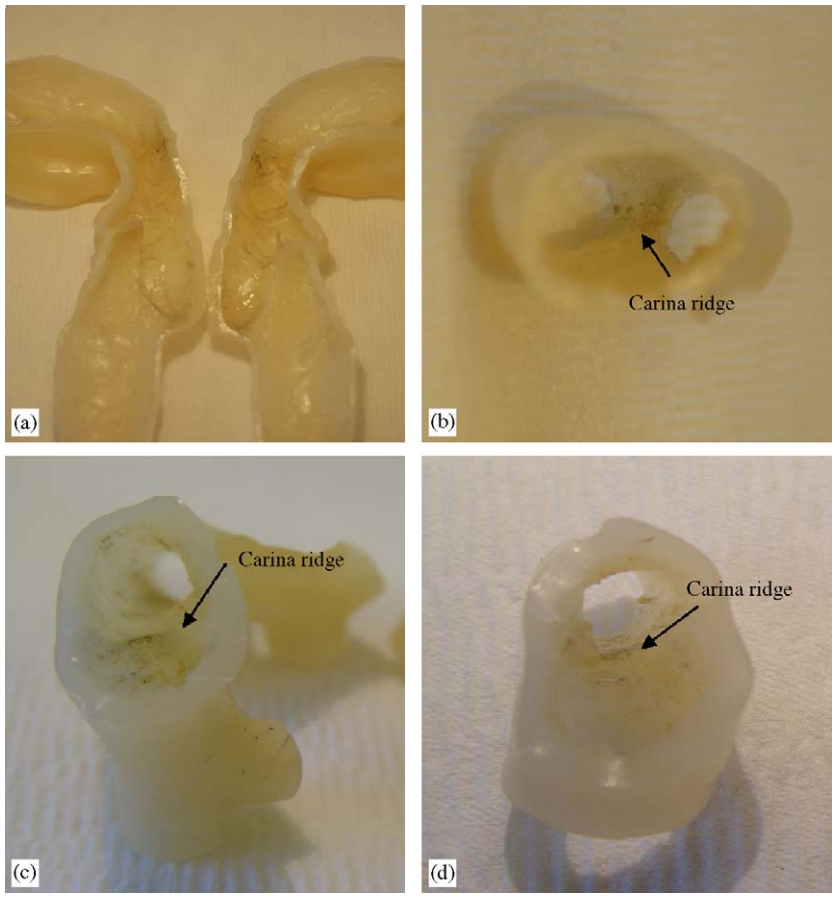

Fig. 4. The preferred deposition sites of fiber in the human airway: (a) oral airway, (b) first bifurcation, (c) second bifurcation, and (d) third bifurcation (inspiratory flow rate = 43.5 l/ min).

along the carina ridge. This deposition "hot spot" (carina) agrees well with what was observed by Myojo (1987) and Sussman et al. (1991) in their experiments.

3.2. Deposition pattern

The fiber deposition fractions could be obtained when the information of fiber number and length distributions were acquired for all segments of the replica and the filters. Figs. 5–7 show the fiber deposition patterns for three inspiratory flow rates with combined length categories. The deposition fraction for each region is an average value of three experiments. For a low inspiratory flow rate of 15 l/min (Fig. 5), the deposition pattern indicates that most of the fibers (at least 63%) passed through the entire human airway replica. The passing through percentage decreased as the fiber length increased. Fiber deposition in each region of the replica was all below 10%, and the typical deposition fraction in the bronchial airways was below 2%. Overall, the oral cavity, larynx, and trachea had relatively higher deposition fractions compared to other regions. Long fibers were shown to have a higher deposition fraction than short fibers for any specific region in the human airway.

Fig. 6 shows the deposition pattern for a 43.5 l/min inspiratory flow rate. As can be seen, a considerable percentage of fibers were deposited in the human airway at this inspiratory flow rate. Most of the deposition was at the oropharynx to larynx area and some were at the first bifurcation. Approximately 30% of the short fibers still passed through the replica, but only 15% of the long fibers were able to pass through the replica. The deposition fraction for a specific region basically increased as the fiber length increased, which is similar to Fig. 5. It is worth noting that the deposition fraction in the oropharynx gradually became significant.

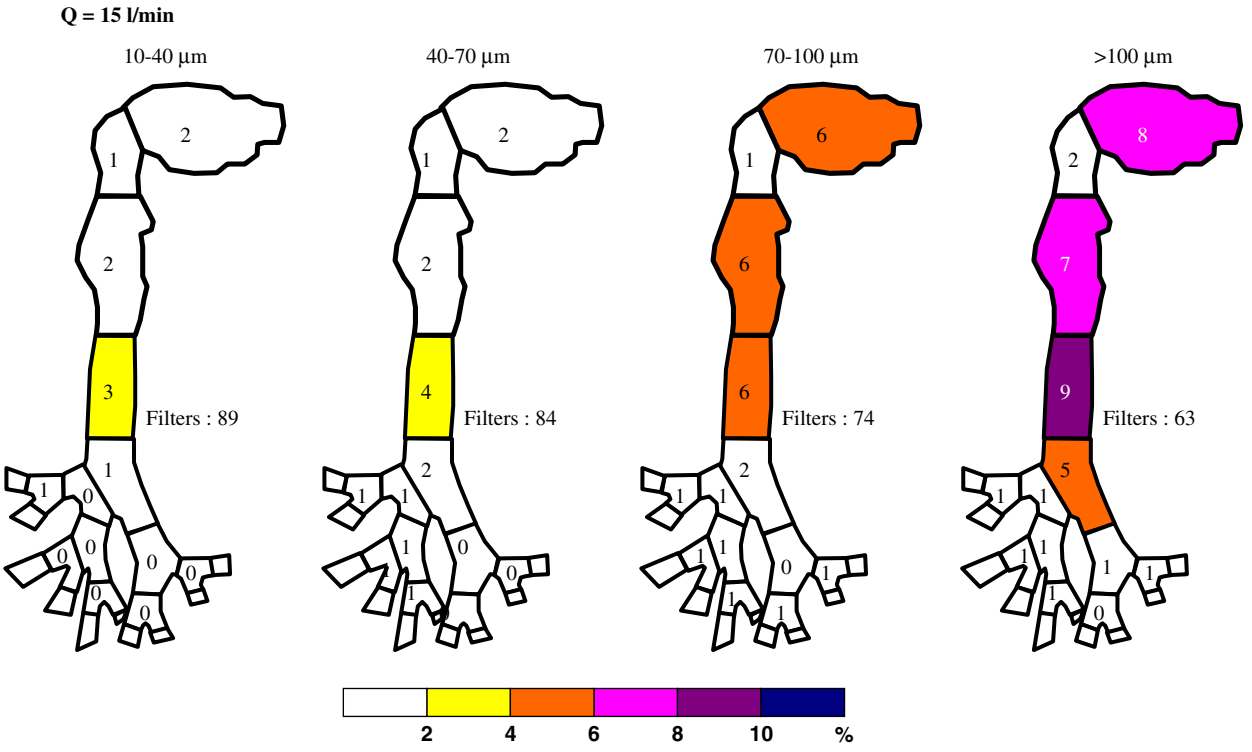

Fig. 5. Fiber deposition map for an inspiratory flow rate of 15 l/min. Deposition fraction is shown in percent (0 corresponds to $< 0.5\%$).

The deposition pattern for a 60 l/min inspiratory flow rate is shown in Fig. 7. As can be seen, similar to that of the 43.5 l/min inspiratory flow rate (Fig. 6), the majority of the fibers were deposited at the area of oropharynx to larynx. The total deposition fraction in this area was around 40–50% for different length categories. However, different from Figs. 5 and 6, the deposition "hot spot" in Fig. 7 shifted from the larynx to the oropharynx. In addition, the fiber deposition in the trachea decreased slightly, which is believed due to the dimensional change of the glottis opening at this inspiratory flow rate. For long fibers ($> 100\,\mu m$), the total deposition in the human airway was larger than 90%, which implies that long fibers had more difficulty passing through the entire replica in high inspiratory flow rate.

4. Discussion

4.1. Deposition mechanism

It was shown in Figs. 5–7, the oropharynx and larynx were found to be the sites of preferred deposition. The oropharynx and larynx are known to be located downstream of an air distortion (the inhaled air experienced a flow direction change from horizontal to vertical). Based on this result, it implies that inertia is an important factor for fiber deposition in the human airway. Impaction, which is closely related to inertia, is therefore the primary deposition mechanism.

Fig. 8 shows deposition trends in the human airway for fibers in three different deposition scenarios. The deposition scenarios A, B, and C represent fibers in low-, intermediate-, and high-inertia regimes, respectively. The Y-axis shows the deposition fraction and the X-axis represents the regions of the human airway. The second to fourth bifurcations in the X-axis stand for the integrations of regions for the same bifurcation. As can be seen in Fig. 8, the deposition trends basically vary from one to another. The discrepancy of the deposition trend is significant in the upper airway (oral cavity to larynx) and at the filters. In the upper airway, 64% of the fibers in deposition scenario C (high inertia) deposited in the oral to larynx area, and the deposition peak was located at oropharynx. Only a small number of fibers were found

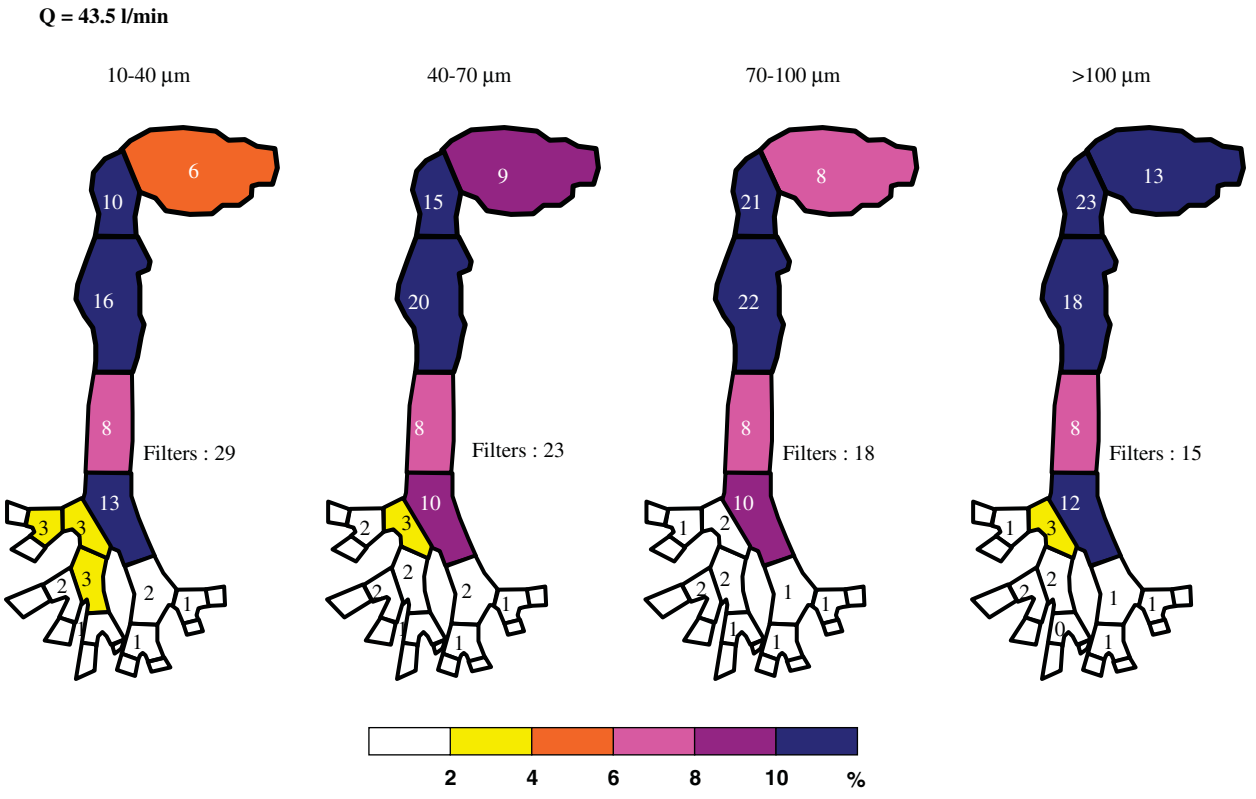

Fig. 6. Fiber deposition map for an inspiratory flow rate of 43.5 l/min. Deposition fraction is shown in percent (0 corresponds to < 0.5%).

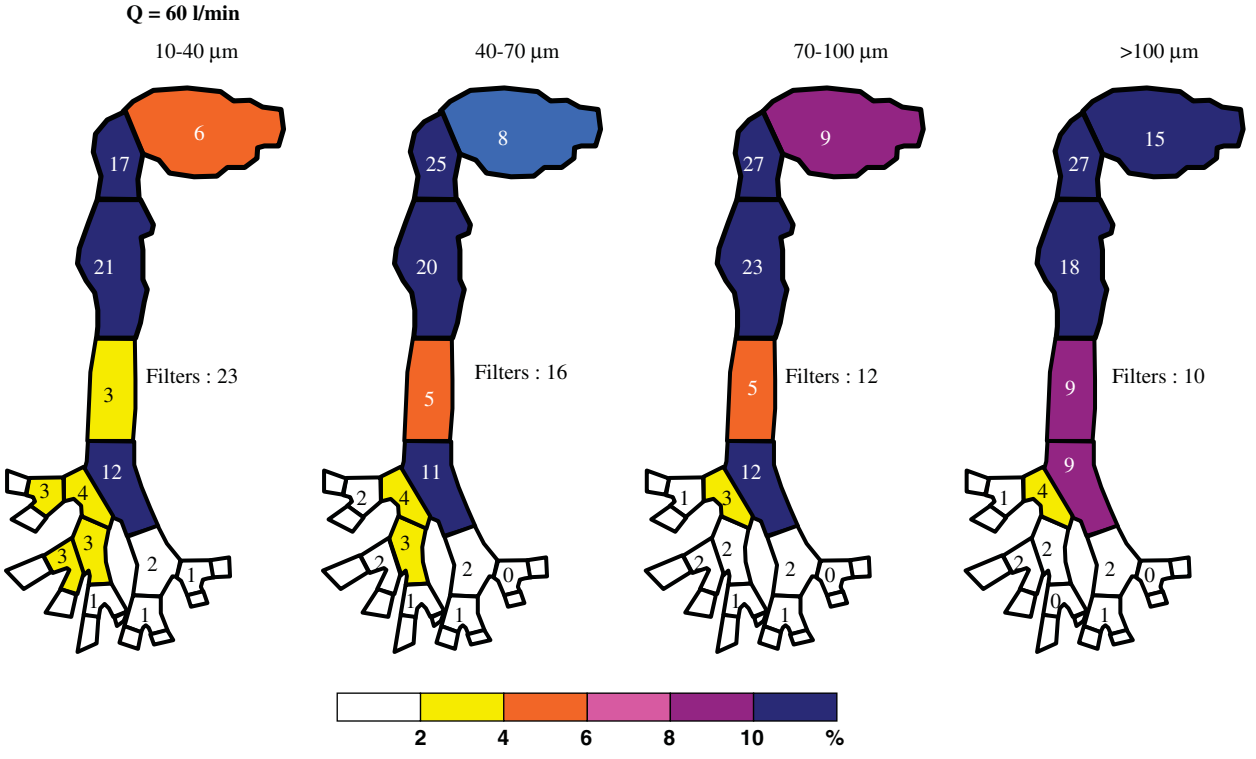

Fig. 7. Fiber deposition map for an inspiratory flow rate of 60 l/min. Deposition fraction is shown in percent (0 corresponds to < 0.5%).

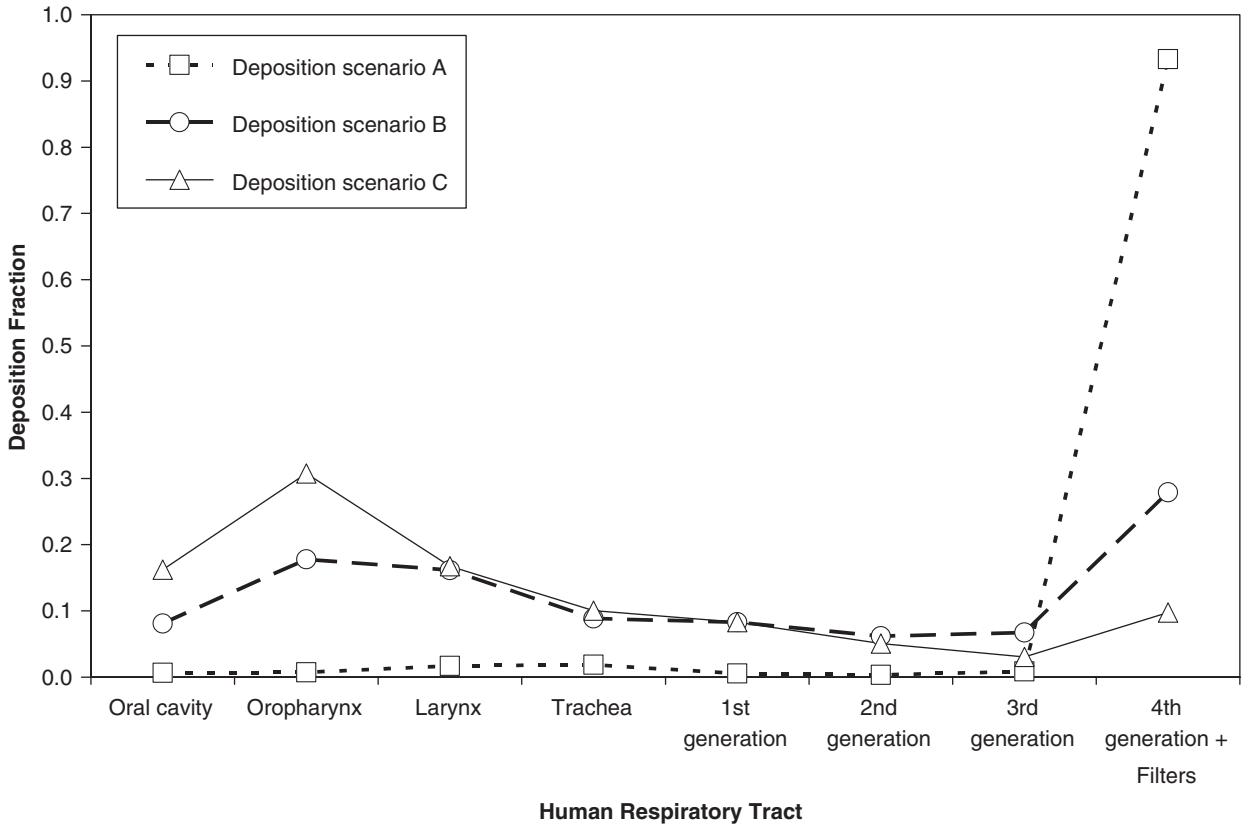

Fig. 8. The deposition trend of fiber in the human airway for different deposition scenarios (deposition scenario A: fibers 10–20 μm with an inspiratory flow rate of 15 l/min; deposition scenario B: fibers 60–70 μm with an inspiratory flow rate of 43.5 l/min; deposition scenario C: fibers > 200 μm with an inspiratory flow rate of 60 l/min).

on the filter. For deposition scenario A (low inertia), low deposition fractions were shown in the upper airway, and the deposition fractions were all below 2%. Most of the fibers in deposition scenario A passed through the replica and were collected on the filters. The filter collection percentage for fibers in this deposition scenario is larger than 90%. The deposition phenomena for deposition scenarios A and C could be explained as follows: when air is inhaled through the oral airway, it experiences a 90° turn from a horizontal to a vertical direction at the oropharynx. Fibers having low inertia (deposition scenario A) can follow the air flow closely and make the turn easily to avoid impacting on the bend area at the oropharynx. Therefore, few low-inertia fibers deposited around the oropharynx as shown in Fig. 8; and most of the low-inertia fibers could pass beyond the oropharynx, even the entire airway, and then deposit on the filters. On the other hand, fibers with high inertia (deposition scenario C) have difficulty flying along with the air when the air flow is distorted. As a result, they were not able to make the turn easily with the airstream, and most of these high-inertia fibers impacted on the dorsal side of the oropharynx (Fig. 4a). The deposition fraction at the oropharynx is, therefore, comparatively large as shown in Fig. 8.

The deposition phenomenon is considerably different in the lower airway (tracheobronchial airways). As can be seen in Fig. 8, the deposition trends for these three deposition scenarios in the first to third bifurcations were similar, and the deposition fractions in each bifurcation were all below 10% regardless of deposition scenario. Theoretically, it is well known that fiber deposition in the tracheobronchial airways is not caused by impaction solely. The interception mechanism might be involved in the deposition process because when a fiber passes a bifurcation, its elongated body has more of a chance to be blocked by the carina ridge of the bifurcation. Thus, the fiber deposition mechanism in human tracheobronchial airways should be impaction and interception together. However, some theoretical calculations (Asgharian, 1988; Asgharian, Zhang, & Fang, 1997; Chen & Yu, 1991) and experimental observation (Myojo, 1987) have shown that fibers tend to align themselves with the flow direction. Moreover, in this study, the diameters of the

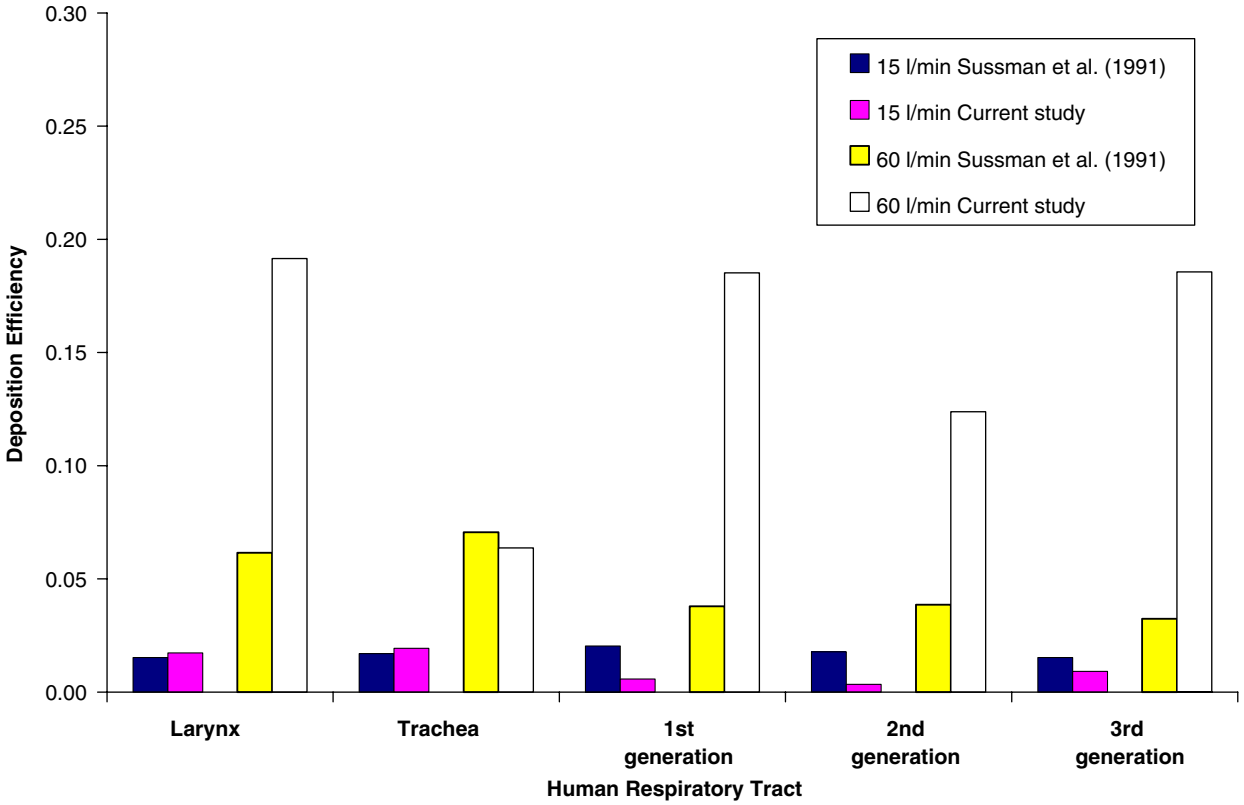

Fig. 9. Comparison of fiber deposition efficiencies for inspiratory flow rates of 15 and 60 l/min (fiber length: 10–20 μm).

tracheobronchial bifurcations (5–15 mm) are much larger than the general length of the fiber (0.01–0.15 mm). As a result, there might not be too many fibers being intercepted by the carina when flying through a bifurcation. Therefore, it could be assumed that interception is not a critical deposition mechanism in this study. The major deposition mechanism in the tracheobronchial airways is believed to be impaction as well. The interception would be an important deposition mechanism when the diameter of the bifurcation has a similar scale as the fiber length. The low deposition fraction shown in the tracheobronchial airways in Fig. 8 is mainly due to the nature of the difficulty for fibers to impact on the carina ridge when aligning with the air flow.

The deposition trend of deposition scenario B (intermediate inertia) has a combined characteristic from both deposition scenario A (low inertia) and deposition scenario C (high inertia). As can be seen in Fig. 8, many fibers in deposition scenario B were deposited in the oral cavity to trachea area, which is a similar result as in deposition scenario C. On the other hand, a substantial portion of fibers were also found to pass through the entire replica, which is similar to the result of deposition scenario A. In general, most of the deposition fractions for deposition scenario B were found in between the values of the other deposition scenarios.

4.2. Comparison of fiber deposition in the human tracheobronchial airway

Sussman et al. (1991) conducted experiments of asbestos fiber deposition in a realistic human tracheobronchial airway replica. The replica used included the trachea, the bronchial airways up to the ninth bifurcation, and an artificial larynx (oral airway not included). In their research, the sites of preferred deposition were determined and the deposition efficiency was reported for each region of the airway up to the sixth bifurcation (in Sussman et al., 1991, the defined "generations" were actually the "bifurcations" in this study). Fig. 9 shows a comparison of the deposition efficiency for the equivalent region in the tracheobronchial airways between Sussman et al. (1991) and this study. The deposition

efficiency in both studies was calculated by

$$e = N_{\text{deposit}(i,j)}/N_{\text{enter}(i,j)}, \tag{5}$$

where $N_{\text{deposit}(i,j)}$ represents the total number of fibers in length category j that deposited in the airway region i, and $N_{\text{enter}(i,j)}$ is the total number of fibers, in the same length category j, entered that region i. The comparison was made only for fibers in the 10–20 μm length category with an inspiratory flow rate of 15 and 60 l/min. As can be seen in Fig. 9, the deposition efficiencies for both experiments in the inspiratory flow rate of 15 l/min were in a similar data range and were all below 2.5%. The deposition efficiencies agree well in the larynx and trachea sections but are slightly discrepant in the tracheobronchial airways, especially in the first and second bifurcations. Since the fiber inertia is low at this inspiratory flow rate for both studies, this slight disagreement might be due to the nature of the individual variety of the human lung and a possible reason for the lack of the effects of the oral cavity, oropharynx, and the actual larynx.

For the inspiratory flow rate of 60 l/min, the deposition efficiencies are much larger than those of the inspiratory flow rate of 15 l/min. The discrepancy of the deposition efficiency between this study and Sussman et al. (1991) was found to be substantial. Almost all deposition efficiencies in our study are larger than those of Sussman et al. (1991). This difference could be explained also by the "inertia rationale" as mentioned in Section 4.1. As reported by Sussman et al. (1991), the median fiber diameter of the asbestos fiber used was 0.3 μm. These asbestos fibers were preselected before delivered into the lung cast, and the aerodynamic diameter, d_{ae} was shown in the range of 0.9–1.1 μm. In contrast, the carbon fibers used in this study have the d_{ae} ranging from 7.9–9.7 μm for a 10–20 μm long fiber in question (all orientations considered). Therefore, under the inspiratory flow rate of 60 l/min, the fiber inertia in this study is considerably higher than that in Sussman et al. (1991). As a result, the higher deposition efficiency in this study is reasonable.

4.3. Deposition of fiber in the oral airway

The oral airway is the main entrance for inhaled air when people are performing moderate to heavy work or exercise. Certain people even use the oral airway as the major airway for breathing. Therefore, there is a high possibility for toxic aerosol to enter the human airway through the oral airway. Numerous deposition studies have been carried out in our laboratory for human airways with spherical particles (Cheng et al., 1999; Cheng, Fu, Yazzie, & Zhou, 2001; Cheng et al., 2003; Zhou & Cheng, 2005). In those studies, the deposition fractions as well as the deposition efficiencies for several regions in the human airway were acquired. Here, the fiber deposition efficiency obtained in this study is compared with those spherical particle data reported by Cheng et al. (1999). The comparison is focused on the oral airway since the oral airways used in these two studies were made from the same production mould. Fig. 10 shows the fiber deposition efficiency in the oral airway as a function of the impaction parameter for fibers and spherical particles. The deposition efficiency was calculated by Eq. (6), and $d_{\text{ae}(\|)}$ was used as the d_{ae} for fiber to obtain the impaction parameter $d_{\text{ae}}^2 Q$. Also shown in Fig. 10, for the purpose of comparison, are the deposition efficiencies of fibers and spherical particles in the human nasal airway (Cheng, Holmes, et al., 2001; Su & Cheng, 2005). The oral airway defined in this study includes the oral cavity and oropharynx. The nasal airway includes from nostril to nasopharynx. As can be seen in Fig. 10, in general, the deposition efficiencies of fibers and spherical particles in the oral airway are much less than those in the nasal airway. For a given value of impaction parameter around 2×10^4–3×10^4, the difference of the deposition efficiency between oral and nasal airways could be as large as 90%.

In Fig. 10, the fiber deposition efficiency in the oral airway increases as the impaction parameter ($d_{\text{ae}}^2 Q$) increases, which reconfirms that impaction is the major deposition mechanism. In comparison with the value of the deposition efficiency between fibers and spherical particles in the oral airway, the deposition efficiency of fibers is shown to be significantly lower than that of spherical particles. This result agrees with what was found in Su and Cheng (2005) for the nasal airway (also shown in Fig. 10), and suggests that if a fiber and a spherical particle have the same aerodynamic diameter and both are delivered into the human oral or nasal airway, fibers will pass through the airway relatively easier than the spherical particles do, which implies that inhaled fiber (no matter by oral or nasal airway) may have more of a chance of entering the lower airway, i.e., the deep lung, compared with spherical particles.

As mentioned above, many studies have documented that fibers tend to align themselves to the flow direction when flying in the air flow. In this way, fibers could follow closely with the air flow, make a turn relatively easier, and then pass through the oral or nasal airway. This might provide an explanation for the difference of the deposition efficiencies shown in Fig. 10.

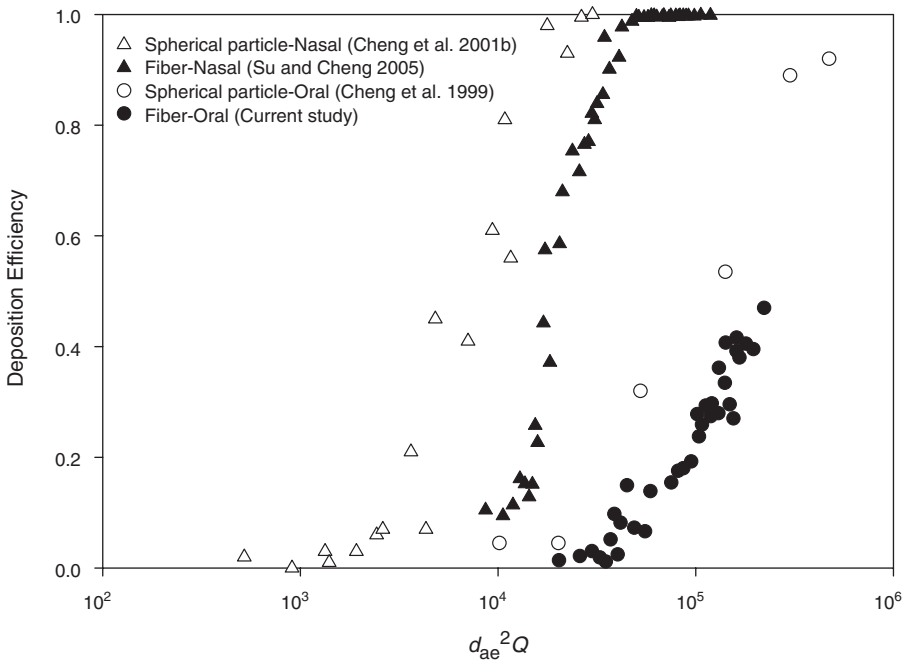

Fig. 10. Comparison of deposition efficiencies between fibers and spherical particles in human oral airway and nasal airway.

5. Conclusion

In this study, experiments were conducted for investigating the effect of fiber dimension and inertia on the deposition pattern in the human airway. Aerosolized carbon fiber was delivered into a human airway replica at constant inspiratory flow rates of 15–60 l/min. The deposition results obtained showed a set of deposition patterns and deposition trends for the human airway. It was indicated that impaction is the dominant deposition mechanism. The oropharynx was found to be the site of preferred deposition for fibers with high inertia. Most fibers with low inertia were found to pass through the entire replica easily. In comparison with fiber deposition in the oral and nasal airway, the fiber deposition efficiency in the oral airway was shown to be much smaller than that in the nasal airway. Besides, the deposition efficiency of fiber was presented generally lower than that of spherical particles in both oral and nasal airways.

Since fiber deposition in the human airway is believed to be a function of the physical characteristic of the fiber, the deposition information obtained from this study is useful in assessing the exposure dosimetry as well as predicting the deposition pattern for other types of fibers, including newly developed MMVFs.

Acknowledgments

The authors are grateful to W. T. Fan for technical assistance, and V. Fisher for reviewing this manuscript. This project is sponsored by NIOSH Grant R01 OH003900.

References

Asgharian, B. (1988). *Theoretical deposition of fibrous particles in the respiratory system of human and rats.* Doctoral dissertation, University of New York at Buffalo, Buffalo.

Asgharian, B., Zhang, L., & Fang, C. P. (1997). Theoretical calculations of the collection efficiency of spherical particle and fibers in an impactor. *Journal of Aerosol Science*, *2*, 277–287.

Bernstein, D. M., Riego Sintes, J. M., Ersboell, B. K., & Kunert, J. (2001). Biopersistence of synthetic mineral fibers as a predictor of chronic intraperitoneal injection tumor response in rats. *Inhalation Toxicology*, *13*, 851–875.

Chen, B. T., Yeh, H. C., & Hobbs, C. H. (1993). Size classification of carbon fiber aerosols. *Aerosol Science and Technology*, *19*, 109–120.

Chen, Y. K., & Yu, C. P. (1991). Sedimentation of fibers from laminar flows in a horizontal circular duct. *Aerosol Science and Technology*, *14*, 343–347.

Cheng, Y. S., Fu, C. S., Yazzie, D., & Zhou, Y. (2001). Respiratory deposition patterns of salbutamol pMDI with CFC and HFA-134a formulations in a human airway replica. *Journal of Aerosol Medicine*, *14*, 255–266.

Cheng, Y. S., Holmes, T. D., Gao, J., Guilmette, R. A., Li, S., Surakitbanharn, Y. et al. (2001). Characterization of nasal spray pumps and deposition pattern in a replica of human nasal airway. *Journal of Aerosol Medicine*, *14*, 267–280.

Cheng, Y. S., Powell, Q. H., Smith, S. M., & Johnson, N. F. (1995). Silicon carbide whiskers: Characterization and aerodynamic behavior. *American Industrial Hygiene Association Journal*, *56*, 970–978.

Cheng, Y. S., Smith, S. M., & Yeh, H. C. (1997). Deposition of ultrafine particles in human tracheobronchial airways. *The Annals of Occupational Hygiene*, *41*(Suppl. 1), 714–718.

Cheng, Y. S., Yazzie, D., Gao, J., Muggli, D., Etter, J., & Rosenthal, G. J. (2003). Particle characteristics and lung deposition patterns in a human airway replica of a dry powder formulation of polylactic acid produced using supercritical fluid technology. *Journal of Aerosol Medicine*, *16*(1), 65–73.

Cheng, Y. S., Yeh, H. C., Guilmette, R. A., Simpson, S. Q., Cheng, K. H., & Swift, D. L. (1996). Nasal deposition of ultrafine particles in human volunteers and its relationship to airway geometry. *Aerosol Science and Technology*, *25*, 274–291.

Cheng, Y. S., Zhou, Y., & Chen, B. T. (1999). Particle deposition in a cast of human oral airways. *Aerosol Science and Technology*, *31*, 286–300.

Cohen, B. S., Sussman, R. G., & Lippmann, M. (1990). Ultrafine particle deposition in a human tracheobronchial cast. *Aerosol Science and Technology*, *12*, 1082–1091.

Hesterberg, T. W., & Hart, G. A. (2001). Synthetic vitreous fibers: A review of toxicology research and its impact on hazard classification. *Critical Reviews in Toxicology*, *31*, 1–53.

IARC (International Agency for Research on Cancer). (2002). *IARC monographs on the evaluation of carcinogenic risks to humans*, Vol. 81. *Man-made vitreous fibers*. Lyon: IARC Press.

Kamstrup, O., Ellehauge, A., Collier, C. G., & Davis, J. M. G. (2002). Carcinogenicity studies after intraperitoneal injection of two types of stone wool fibres in rats. *The Annals of Occupational Hygiene*, *46*(2), 135–142.

Lippmann, M. (1990). Effects of fiber characteristics on lung deposition, retention, and disease. *Environmental Health Perspectives*, *88*, 311–317.

Martonen, T. B., & Lowe, J. (1983). Assessment of aerosol deposition patterns in human respiratory tract casts. *Aerosols in the mining and industrial work environments:*(pp. 151–164). Vol. 1, Ann Arbor, MI: Ann Arbor Science.

Myojo, T. (1987). Deposition of fibrous aerosol in model bifurcating tubes. *Journal of Aerosol Science*, *1*, 337–347.

NIOSH (1994). Asbestos and other fibers by PCM. In *NIOSH manual of analytical method*.

Stöber, W. (1972). Dynamic shape factors of nonspherical aerosol particles. in: T. Mercer et al. (Ed.), *Assessment of airborne particles* (pp. 249–289). Springfield, IL: Charles C. Thomas Publisher.

Stöber, W., Flachsbart, H., & Hochrainer, D. (1970). The aerodynamic diameter of latex aggregates and asbestos fibres. *Staub-Reinhalt Luft*, *30*, 1–12.

Su, W. C., & Cheng, Y. S. (2005). Deposition of fiber in the human nasal airway. *Aerosol Science and Technology*, *39*, 888–901.

Sussman, R. G., Cohen, B. S., & Lippmann, M. (1991). Asbestos fiber deposition in human tracheobronchial cast. I. Experimental. *Inhalation Toxicology*, *3*, 145–160.

Timbrell, V. (1982). Deposition and retention of fibers in human lung. *The Annals of Occupational Hygiene*, *26*, 347–369.

Willeke, K., & Baron, P. A. (1993). *Aerosol measurement*. New York: Wiley, pp. 565.

Zhou, Y., & Cheng, Y. C. (2005). Particle deposition in a cast of human tracheobronchial airways. *Aerosol Science and Technology*, *39*, 492–500.